Research Square

Preprints are preliminary reports that have not undergone peer review.
They should not be considered conclusive, used to inform clinical practice,
or referenced by the media as validated information.

Significance of mucin type glucosaminyl (N-acetyl) transferase 3 expression in lung squamous cell carcinoma

Yu-Jun Chen
Guangxi Medical University
Li Gao
Guangxi Medical University First Affiliated Hospital
Rui Zhang
Guangxi Medical University First Affiliated Hospital
Gang Chen
Guangxi Medical University First Affiliated Hospital
Zhen-bo Feng (fengzhenbo_gxmu@163.com)
The First Affiliated Hospital of Guangxi Medical University https://orcid.org/0000-0001-6361-4198
Yong-Xiang Zhao
Guangxi Medical University

Research

Keywords: GCNT3, LUSC, tissue microarray, IHC, RNA-seq

Posted Date: January 13th, 2021

DOI: https://doi.org/10.21203/rs.3.rs-142867/v1

License: This work is licensed under a Creative Commons Attribution 4.0 International License.
Read Full License

Abstract

Background: The clinical significance and role of glycan synthase glucosamine (N-acetyl) transferase 3 (GCNT3) has not been investigated in lung squamous cell carcinoma (LUSC).

Materials & Methods: In the present study, multiple detection technologies including tissue microarrays, external microarrays and RNA-seq were adopted for evaluating the clinic-pathological significance of GCNT3 in 1632 LUSC samples and 1478 non-cancer samples. Standard mean difference and hazard ratio value were calculated from all included datasets for assessing differential expression and prognostic value of GCNT3 in LUSC. The molecular basis underlying GCNT3 in LUSC was also explored through methylation level, genetic mutation and functional enrichment analysis of GCNT3-correlated genes in LUSC.

Results: GCNT3 was obviously upregulated in LUSC samples. GCNT3 overexpression exerted unfavorable impact on the progression-free survival and overall survival of LUSC patients from GSE29013. The mRNA expression of GCNT3 was negatively correlated with methylation level of GCNT3 in LUSC and the predominant type of genetic alteration for GCNT3 in LUSC was mRNA high. Genes correlated with GCNT3 in LUSC mainly assembled in pathways such as adherens junction, p53 signaling pathway, protein digestion and absorption pathway.

Conclusions: In conclusion, overexpressed GCNT3 had clinical potential as therapeutic target for LUSC.

Introduction

Lung cancer continues to be the principle cause of mortality related to cancer worldwide [1] and one of the common types of non-small cell lung cancer is lung squamous cell carcinoma (LUSC)[2]. Although multiple treatment options based on genome targeting including gefitinib, erlotinib and bevacizumab have been developed for patients with lung adenocarcinoma, LUSC patients showed poor response to these regimen and few therapeutic options were available for LUSC patients [3]. The prognosis of LUSC patients remains unsatisfactory and the survival time of more than 90% of LUSC patients with advanced metastasis was less than 5 years [4]. Therefore, there is an imperative to seek characteristic marker of LUSC for better clinical management of LUSC.

Glycan synthase glucosamine (N-acetyl) transferase 3 (GCNT3) is a glycosyltransferase enzyme that played key roles in the catalyzation of core 2, core 4 O-glycans and and I branches [5]. GCNT3 was closely related to a range of biological processes including inflammatory and immune responses [6]. Dysregulated GCNT3 producing excessive mucins caused perturbation to cellular glycosylation, which is a hallmark of human cancers [7, 8]. Previous researchers have discovered upregulation of GCNT3 in several human cancers such as EBV-associated gastric cancer, pancreatic cancer and non-small cell lung cancer [6, 7, 9]. Qian Li et al. demonstrated that inhibiting GCNT3 expression through miR-302b-3p could diminish the proliferation, migration and invasion of non-small cell lung cancer cells [7]. CRISPR-mediated knockout of

GCNT3 conducted by Chinthalapally V Rao et al. reduced mucin and mitigated aggressive biological phenotype in pancreatic cancer [6]. In gastric cancer, miR-BART1-5p targets GCNT3 to suppress proliferative and migratory abilities of EBV-associated gastric cancer cells. Until now, GCNT3 in LUSC has not been investigated [9].

Herein, multiple detection technologies including tissue microarrays, external microarrays and RNA-seq were adopted in the current work for a system assessment of the clinic-pathological and prognostic significance of GCNT3 in LUSC. The molecular basis underlying GCNT3 in LUSC was also explored through genetic mutation, methylation level and functional enrichment analysis of GCNT3-correlated genes in LUSC.

Materials And Methods

Tissue microarray

Tissue microarrays including LUC481, LUC482, LUC483, LUC1021, LUC1501, LUC1502, LUC1503, LUC1506, LUC1601 and LUC1602 were provided by Pantomics, Inc. (Guilin, China). Three pairs of samples from the First Affiliated Hospital of Guangxi Medical University were additionally included for tissue microarray. A total of 119 non-cancerous lung samples and 250 LUSC samples were used for tissue microarray. The study was approved by the Ethics Committee of the First Affiliated Hospital of Guangxi Medical University with informed consent signed by all patients. Tissue sections were stained against GCNT3 using the first antibody (AB227972, Abcam, Cambridge, USA) at 1/500 dilution. Subsequently, the tissue sections were incubated with the second antibody (horseradish peroxidase). Two pathologists (Gang Chen and Zhen-Bo Feng) independently evaluated immunohistochemistry (IHC) results of all slides using the semi-quantitative scoring system. Scores of 0, 1, 2 and 3 corresponded to negative, weak, moderate and strong staining intensity, respectively; and the staining proportion was recorded as 0 (< 10%), 1 (11–25%), 2 (26–50%), 3 (51–75%), and 4 (76–100%). Multiply of staining intensity and proportion determines the final immunoreactivity score.

GCNT3 expression in all pan-squamous cell carcinomas

Curious about whether the GCNT3 overexpression is tumor-specific, or whether the expression level of GCNT3 in other squamous cell carcinomas was similar with that in LUSC, we analyzed GCNT3 expression profile in pan-squamous cell carcinoma. GCNT3 expression in cervical squamous cell carcinoma (CESC), esophageal carcinoma (ESCA), head and neck squamous cell carcinoma (HNSC), LUSC as well as the normal tissues were checked via Firebrowse (http://www.firebrowse.org/).

Integration of tissue microarray, external microarrays and RNA-seq datasets for comprehensive GCNT3 expression analysis

Fragments per kilobase per million (FPKM) gene expression matrix and clinical information of LUSC patients from the cancer genome atlas (TCGA) were acquired from GDC data portal

(https://portal.gdc.cancer.gov/repository). The transcripts per kilobase million (TPM) gene expression matrix of normal lung tissues from GTEx database were additionally downloaded. Datasets from TCGA and GTEx (502 LUSC samples and 476 non cancer samples) were combined and the gene expression matrix was standardized with the algorithm of log2 (TPM + 0.001). Microarrays from gene expression omnibus (GEO) (https://www.ncbi.nlm.nih.gov/gds/?term=) or ArrayExpress (https://www.ebi.ac.uk/arrayexpress/) databases covering expression data of GCNT3 in at least three human LUSC and non cancer lung samples published before August 3rd, 2020 were also enrolled for comprehensive expression analysis.

Methods of extracting and processing expression data of GCNT3 from microarrays were clearly stated before [10]. The IHC scores of GCNT3 in LUSC and non-cancer tissues were incorporated into the expression matrix from all external microarrays and RNA-seq datasets for calculation of the standardized mean difference (SMD) and 95% confidence interval (CI) of GCNT3 expression between LUSC and non-cancer samples. Random-effect model of meta package in R software v.3.6.1 was applied for calculating SMD. The summarized receiver's operating characteristics (SROC) curves were drawn by stata v.14.0 for assessing the ability of GCNT3 to differentiate LUSC from non-cancer samples [11].

Survival analysis

RNA-seq or microarrays from TCGA, GEO and ArrayExpress databases with survival information of LUSC patients and GCNT3 expression data in LUSC tissues were collected. Kaplan Meier survival curves with log-rank P value were plotted by GraphpadPrism v.8.0.1 to analyze the effect of GCNT3 expression on survival of LUSC patients from included datasets. Cutoff value for dividing LUSC patients was the median expression value of GCNT3 and $P < 0.05$ was statistically significant. HRs calculated from different datasets were combined into an overall index with random-effect model of meta package in R software v.3.6.1.

Alteration and methylation status of GCNT3 in LUSC

Catalogue of Somatic Mutations in Cancer (COSMIC) and cBioPortal databases were employed for querying mutation types of GCNT3 and genetic alteration profile of GCNT3 in 178 LUSC samples with mutation data from TCGA database. The correlation between GCNT3 methylation level in HM450 and mRNA expression Z-scores of GCNT3 in LUSC was analyzed via cBioPortal.

Functional enrichment analysis for GCNT3-correlated genes in LUSC

Gene expression matrix of LUSC versus non-cancer lung tissues from RNA-seq dataset of TCGA database and microarrays with gene expression matrix of LUSC from GEO or ArrayExpress databases was prepared and normalized using limma package in R software v.3.6.1. Differential expression analysis was conducted for each expression matrix with limma package in R software v.3.6.1 and genes displaying simultaneous upregulation or downregulation (log2FC > 1&adjusted P < 0.05; log2FC<-1&adjusted P < 0.05) in no less than ten datasets of LUSC were defined as differentially expressed genes (DEGs) of

LUSC. Correlation analysis of GCNT3 expression and other genes was performed using the Pearson correlation method of psych package in R software v.3.6.1 for each eligible dataset. The intersection of the above defined upregulated DEGs and genes showed positive relationship with GCNT3 ($r > 0$, adjusted $P < 0.05$) were defined as genes positively correlated with GCNT3 in LUSC; the intersection of the above defined downregulated DEGs and genes showed negative relationship with GCNT3 were defined as genes negatively correlated with GCNT3 in LUSC. Gene ontology (GO) and Kyoto Encyclopedia of Genes and Genomes (KEGG) pathway analysis was performed for genes positively or negatively correlated with GCNT3 via ClusterProfiler package in R software v.3.6.1. $P < 0.05$ was the threshold of significant GO and KEGG terms.

Statistical analysis

SPSS 16.0 was employed for the statistical analysis of in-house tissue microarray data. GCNT3 expression in LUSC and non-cancer tissues was presented as mean ± standard deviation. Because of the non-normal distribution of GCNT3 expression in 250 LUSC cases and 119 non-cancer cases of tissue microarrays, Mann-Whitney and Kruskal-Wallis tests were used for comparing GCNT3 protein expression in different clinical parameter groups. Violin plots visualizing GCNT3 expression in LUSC and non-cancer tissues as well as ROC curves for each dataset was drawn with ggplot2 and pROC packages in R software v.3.6.1. $P < 0.05$ was considered as statistically significant.

Results

GCNT3 expression in LUSC from tissue microarrays

The 250 LUSC samples involved in tissue microarrays consist of 23 females and 224 males with an average age of 58; the 119 non-cancer lung samples involved in tissue microarrays consist of 13 females and 103 males with an average age of 56 (GaoTable1). According to the results from tissue microarrays, GCNT3 was significantly upregulated in LUSC tissues (10.888 ± 2.350) compared with non-cancer tissues (3.429 ± 1.565) ($P < 0.001$) (GaoFigure1 and Supplementary Fig. 1) (GaoTable1). Images of IHC staining confirmed medium or strong immunoreactivity of GCNT3 in cancer nests of LUSC tissues while weak or even negative immunoreactivity was presented in non-cancer lung tissues (GaoFigure2). Statistical analysis of clinic-pathological data indicated that GCNT3 expression in LUSC patients with early T stage (1–2) and higher grade (11.018 ± 2.174, 11.491 ± 1.543) was remarkably higher than that in LUSC patients with advanced T stage (3–4) and lower grade (9.714 ± 3.343, 8.962 ± 3.509) ($P = 0.024$, $P < 0.001$) (GaoTable1).

GCNT3 expression in pan-squamous cell carcinoma

From the perspective of pan-squamous cell carcinoma, GCNT3 was overexpressed in the majority of squamous cell carcinomas (CESC, ESCA and LUSC) except for HNSC (GaoFigure3).

GCNT3 overexpression in LUSC validated by integrated data of tissue microarray, external RNA-seq and microarrays

Detailed flowchart of selecting eligible RNA-seq and microarray datasets for comprehensive expression analysis was summarized in Supplementary Fig. 2. A total of 27 microarrays from GEO database and two microarrays from ArrayExpress database were included. Basic information of these datasets was given in Supplementary Table 1. The amalgamation of tissue microarray, and external microarrays and RNA-seq datasets contained huge samples of 1632 LUSC cases and 1478 non-cancer cases. Violin plots for differential GCNT3 expression and ROC curves for distinguishing capacity of GCNT3 in all included datasets revealed obvious overexpression of GCNT3 in LUSC and moderate discrimination ability of GCNT3 overexpression in most datasets (GaoFigure1 and Supplementary Fig. 1). Forest plot of SMD merged from all included datasets supported overexpression of GCNT3 in LUSC (SMD = 0.57, 95%CI = 0.15–0.99) (GaoFigure4) and SROC curves generated from the diagnostic data of all included datasets corroborated moderate performance of GCNT3 overexpression in differentiating LUSC from non-cancer tissues (AUC = 0.61, 95%CI = 0.57–0.65) (Supplementary Fig. 3).

Prognostic value of GCNT3 expression for LUSC

Kaplan-Meier survival analysis and log-rank tests were conducted for RNA-seq dataset of TCGA-LUSC project and 15 GEO microarrays (GSE81089, GSE74777, GSE50081, GSE41271, GSE30219, GSE29013, GSE19188, GSE17710, GSE14814, GSE12428, GSE11117, GSE12472, GSE4573, GSE8894 and GSE5123). GCNT3 overexpression exerted unfavorable impact on the progression-free survival and overall survival of LUSC patients from GSE29013 (HR = 3.288, P = 0.034; HR = 4.776, P = 0.029) GaoFigure5). No significant prognostic results were yielded from other datasets. Prognostic data of overall survival, event-free survival, progression-free survival, recurrence free survival or relapse-free survival from the above included datasets were listed in GaoTable2. Forest plots of pooled HR were divided into subtypes of overall survival, recurrence-free survival and relapse-free survival. The influence of GCNT3 expression on the prognosis of LUSC patients reflected from forest plots were insignificant (Supplementary Fig. 4).

Genetic alteration profile of GCNT3 in LUSC

Record from the OncoPrint module of cBioPortal database showed two cases of missense mutation and six cases with high mRNA in 178 LUSC cases from TCGA database (GaoFigure6), which suggested that the predominant type of genetic alteration for GCNT3 was high mRNA in LUSC. No indels (insertion and deletions) and synonymous mutations of GCNT3 in LUSC were found in other databases. The mRNA expression of GCNT3 was negatively correlated with methylation level of GCNT3 ($r=-0.21$, $P < 0.001$) in LUSC

Functional enrichment analysis for GCNT3-correlated genes in LUSC

Differential expression analysis and expression correlation analysis were performed on RNA-seq dataset from TCGA database, in-house microarray and 34 external microarrays with gene expression matrix of

LUSC (E-MTAB-5231, E-MTAB-8615, GSE103512, GSE10937, GSE11117, GSE11969, GSE12428, GSE12472, GSE135304, GSE19188, GSE1987, GSE2088, GSE21933, GSE27489, GSE27553, GSE29249, GSE30219, GSE31446, GSE31552, GSE32036-GPL6884, GSE3268, GSE33479, GSE33532, GSE40275, GSE4824-GPL96, GSE4824-GPL97, GSE49155, GSE6044, GSE62113, GSE67061-GPL6480, GSE74706, GSE81089, GSE84784 and GSE8569). A total of 48 genes and 51 genes were defined as genes positively correlated with GCNT3 and genes negatively correlated with GCNT3, respectively (Supplementary Fig. 5). Genes positively correlated with GCNT3 in LUSC mainly assembled in biological processes and KEGG pathways such as cornification, skin development, keratinocyte differentiation, amoebiasis pathway, p53 signaling pathway and protein digestion and absorption pathway (GaoFigure7). Gens negatively correlated with GCNT3 in LUSC were actively enrolled in biological processes and KEGG pathways including cardiac chamber development, cardiac septum development, cardiac chamber morphogenesis, tryptophan metabolism pathway, fluid shear stress and atherosclerosis pathway and malaria pathway (GaoFigure8).

Discussion

Utilizing combined detection methods of tissue microarray, RNA-seq and external microarrays, we for the first time declared overexpression of GCNT3 in 1632 LUSC samples versus 1478 non-cancer samples. The molecular mechanism beneath GCNT3 overexpression in LUSC was further explored from various angles including methylation level, genetic alteration profile and functional enrichment analysis of correlated genes.

Data from tissue microarray, external RNA-seq and microarrays unanimously supported overexpression of GCNT3 in LUSC, which guaranteed the convincingness of the results in a large sample pool of 1632 LUSC cases and 1478 non-cancer cases. The incorporated datasets also indicated moderate ability of overexpressed GCNT3 to make a distinction between LUSC and non-cancer lung cancer samples. Due to the lack of sufficient datasets containing GCNT3 expression in body fluid samples of LUSC patients, SROC curves was not created for appraising the diagnostic performance of GCNT3 in body fluid samples of LUSC. Inspection of the clinic-pathological information of LUSC patients from tissue microarrays revealed significant relationship between GCNT3 overexpression and higher clinical grade of LUSC, hinting that GCNT3 might propel the malignant clinical progression of LUSC. Previous researchers have also discovered the participation of GCNT3 in the development of other tumors such as pancreatic cancer and gastric cancer [6, 9]. Chinthalapally V Rao et al. reported that abnormal GCNT3 expression lead to increased mucin production and knockout of GCNT3 in pancreatic cancer cells suppressed proliferation and spheroid formation [6]. The work by Juanjuan Liu et al. demonstrated negative regulatory function of miR-BART1-5p on GCNT3-related carcinogenesis of EBV-associated gastric cancer [9]. The above findings provided possible explanation for the oncogenic impact of GCNT3 on LUSC. The other thing to point out is that GCNT3 expression was higher in LUSC patients with early T stage than in LUSC patients with advanced T stage from tissue microarray, which reflected contradictory implications of clinical

significance. The distribution of GCNT3 expression in different T stages of LUSC patients needed to be further examined in larger studies.

Apart from the differential expression, we also evaluated the prognostic significance of GCNT3 in LUSC through integrating HR values of different survival types from datasets with prognostic information. Although the results from pooled HR bore no statistical significance, we are the first group to comprehensively assess the prognostic value of GCNT3 in LUSC through consolidation of survival data from multiple cohorts.

To gain a better understanding of the molecular basis underlying GCNT3 in LUSC, we queried the correlation between GCNT3 expression and methylation level in LUSC as well as the genetic alteration profile of GCNT3 in LUSC with the purpose of exploring the transcriptional regulation beneath GCNT3 overexpression in LUSC. It could be deduced from the results that GCNT3 overexpression in LUSC might result from hypo-methylation and mutation type of mRNA high. Additionally, Functional enrichment analysis of the correlated genes of GCNT3 also offered valuable clues to the molecular events related to GCNT3 in LUSC. Genes negatively and positively correlated with GCNT3 engaged in different biological processes, cellular component and molecular function. Biological processes clustered by genes positively correlated with GCNT3 were concerned with cardiovascular while genes negatively correlated with GCNT3 were frequently involved in biological processes of keratinization. These results implied that genes negatively and positively correlated with GCNT3 played different roles in GCNT3-centered carcinogenesis of LUSC. Significantly enriched KEGG pathways such as adherens junction, p53 signaling pathway and cell cycle pathway were all tightly bound to the malignant behavior of human cancers [12–14]. Among the above pathways, adherens junction is an intermediate link of epithelial-mesenchymal transition. Qian Li et al. reported that epithelial-mesenchymal transition was activated by miR-302b-3p/GCNT3 axis in non-small cell lung cancer [7], which evidenced the indirect connection between GCNT3 and adherens junction. Despite the functions of GCNT3 in other pathways have not been identified in literature studies, GO and KEGG analysis results of the present work may shed light on GCNT3-centered molecular interaction network in LUSC.

Conclusion

In summary, overexpressed GCNT3 might serve as promising therapeutic biomarker for LUSC. GCNT3 might interplay with correlated genes through certain pathways to exert oncogenic influence on clinical development of LUSC. Nano-particle based treatment of tumor is a hot research field in recent years. It is anticipated that nano-particles targeting GCNT3 might exhibit excellent therapeutic power for LUSC in future days. The encouraging results from the present study would guide us to conduct in vitro or in vivo experiments in future work to further validate the function of GCNT3 on biological processes of LUSC cells and the interaction between GCNT3 and correlated genes in certain pathways.

Declarations

Ethics approval and consent to participate

Ethics approval has been provided in the attachment.

Consent for publication

Not applicable.

Availability of data and materials

All data used to support the findings of this study are included within the article and supplementary materials.

Competing interests

No competing financial interests exist.

Funding

This study was funded by Natural Science Foundation of Guangxi, China (2017GXNSFAA198016), Key Scientific and Technological Research and Development Project in Guangxi Zhuang Autonomous Region, China (AB18126057), Guangxi Degree and Postgraduate Education Reform and Development Research Projects, China (JGY2019050) and Guangxi Zhuang Autonomous Region Health and Family Planning Commission Self-financed Scientific Research Project (Z20180979).

Authors' contributions

Zhen-Bo Feng, Yong-Xiang Zhao and Yu-Jun Chen provided the study design. Rui Zhang and Gang Chen collected clinical samples. Rui Zhang and Gang Chen performed immunohistochemistry experiment. Li Gao and Yu-Jun Chen performed the analyses and calculations. Li Gao and Yu-Jun Chen contributed to the writing of the manuscript. All authors have reviewed and approved of the manuscript prior to submission.

Acknowledgements

The authors thank all the public data sources involved in the current study.

References

1. Bray F, Ferlay J, Soerjomataram I, Siegel RL, Torre LA, Jemal A. Global cancer statistics 2018: GLOBOCAN estimates of incidence and mortality worldwide for 36 cancers in 185 countries. CA Cancer J Clin. Nov 2018;68(6):394-424.
2. Sato T, Yoo S, Kong R, et al. Epigenomic Profiling Discovers Trans-lineage SOX2 Partnerships Driving Tumor Heterogeneity in Lung Squamous Cell Carcinoma. Cancer Res. Dec 15 2019;79(24):6084-

6100.
3. Ito T, Ishii G, Nagai K, et al. Low podoplanin expression of tumor cells predicts poor prognosis in pathological stage IB squamous cell carcinoma of the lung, tissue microarray analysis of 136 patients using 24 antibodies. Lung Cancer. Mar 2009;63(3):418-424.
4. Chen SW, Lu HP, Chen G, et al. Downregulation of miRNA-126-3p is associated with progression of and poor prognosis for lung squamous cell carcinoma. FEBS Open Bio. Jun 29 2020.
5. Fernandez LP, Sanchez-Martinez R, Vargas T, et al. The role of glycosyltransferase enzyme GCNT3 in colon and ovarian cancer prognosis and chemoresistance. Sci Rep. May 31 2018;8(1):8485.
6. Rao CV, Janakiram NB, Madka V, et al. Small-Molecule Inhibition of GCNT3 Disrupts Mucin Biosynthesis and Malignant Cellular Behaviors in Pancreatic Cancer. Cancer Res. Apr 1 2016;76(7):1965-1974.
7. Li Q, Ran P, Zhang X, et al. Downregulation of N-Acetylglucosaminyltransferase GCNT3 by miR-302b-3p Decreases Non-Small Cell Lung Cancer (NSCLC) Cell Proliferation, Migration and Invasion. Cell Physiol Biochem. 2018;50(3):987-1004.
8. Rao CV, Janakiram NB, Mohammed A. Molecular Pathways: Mucins and Drug Delivery in Cancer. Clin Cancer Res. Mar 15 2017;23(6):1373-1378.
9. Liu J, Zhang Y, Liu W, et al. MiR-BART1-5p targets core 2beta-1,6-acetylglucosaminyltransferase GCNT3 to inhibit cell proliferation and migration in EBV-associated gastric cancer. Virology. Feb 2020;541:63-74.
10. Gao L, He RQ, Wu HY, et al. Expression Signature and Role of miR-30d-5p in Non-Small Cell Lung Cancer: a Comprehensive Study Based on in Silico Analysis of Public Databases and in Vitro Experiments. Cell Physiol Biochem. 2018;50(5):1964-1987.
11. Gao L, Li SH, Tian YX, et al. Role of downregulated miR-133a-3p expression in bladder cancer: a bioinformatics study. Onco Targets Ther. 2017;10:3667-3683.
12. Bretz AC, Gittler MP, Charles JP, et al. DeltaNp63 activates the Fanconi anemia DNA repair pathway and limits the efficacy of cisplatin treatment in squamous cell carcinoma. Nucleic Acids Res. Apr 20 2016;44(7):3204-3218.
13. Zhang X, Cheng D, Liu Y, Wu Y, He Z. Gephyrin suppresses lung squamous cell carcinoma development by reducing mTOR pathway activation. Cancer Manag Res. 2019;11:5333-5341.
14. Ramteke A, Ting H, Agarwal C, et al. Exosomes secreted under hypoxia enhance invasiveness and stemness of prostate cancer cells by targeting adherens junction molecules. Mol Carcinog. Jul 2015;54(7):554-565.

Tables

Table 1: The clinic-pathological significance of GCNT3 in lung squamous cell carcinoma.

Clinic-pathological feature		N	GCNT3 relevant expression		
			M ± SD	Z	P
Tissue type	LUSC	250	10.888±2.350	-15.992	<0.001
	Non-cancer	119	3.429±1.565		
Age (years)	<60	141	10.81±2.378	-0.681	0.496
	≥60	106	10.96±2.346		
Gender	Female	23	10.78±2.540	-0.121	0.904
	Male	224	10.88±2.348		
T stage	1-2	218	11.018±2.174	-2.26	0.024
	3-4	28	9.714±3.343		
Lymph node metastasis	No	146	11.041±2.117	-1.055	0.291
	Yes	100	10.62±2.677		
Grade	I	52	8.962±3.509	34.782[a]	<0.001
	II	85	11.247±1.690		
	III	110	11.491±1.543		

Notes: LUSC: lung squamous cell carcinoma; N: number; M: mean; SD: standard deviation; T: tumor size;

[a] Kruskal-Wallis test was used to evaluate the relationship between GCNT3 expression and grade of lung squamous cell carcinoma.

Table 2. Survival information for included RNA-seq and microarray datasets

ID	Survival type	Time unit	Median survival of lung squamous cell carcinoma patients from low GCNT3 expression group	Median survival of lung squamous cellcarcinoma patients from high GCNT3 expression group	HR	P
GSE74777	overall survival	days	4075	4615	0.813	0.499
GSE74777	relpase-free survival	days	-	-	0.836	0.634
GSE50081	overall survival	years	5.96	-	0.797	0.572
GSE50081	relapse-free survival	years	-	-	1.061	0.832
GSE41271	overall survival	days	1889	1253	1.309	0.374
GSE41271	recurrence-free survival	days	1058	-	0.9	0.749
GSE30219	overall survival	months	68	89	0.857	0.605
GSE30219	relapse-free survival	months	104	-	0.686	0.372
GSE29013	progression-free survival	years	4.554	1.046	3.362	0.034
GSE29013	overall survival	years	-	2.779	4.776	0.029
GSE19188	overall survival	months	63.03	29.62	1.726	0.250
GSE17710	overall survival	months	31.05	26.78	0.961	0.908
GSE17710	recurrence-free survival	months	23.43	20.44	0.876	0.684
GSE14814	overall survival	years	-	-	0.707	0.452
GSE12428	overall survival	months	117	105	1.332	0.570
GSE11117	overall survival	days	414	-	0.623	0.531
GSE8894	recurrence-free survival	months	38.67	-	0.640	0.182

GSE12472	overall survival	months	117	93	1.545	0.424
GSE5123	recurrence-free survival	months	61.11	128	0.515	0.067
GSE4573	overall survival	months	64.1	78.9	0.904	0.678
GSE81089	overall survival	days	1935	1932	1.139	0.724
TCGA-LUSC	overall survival	days	1656	1335	1.063	0.701
TCGA-LUSC	event-free survival	days	1912	-	0.721	0.064

Note: HR: hazard ratio; LUSC: lung squamous cell carcinoma

Figures

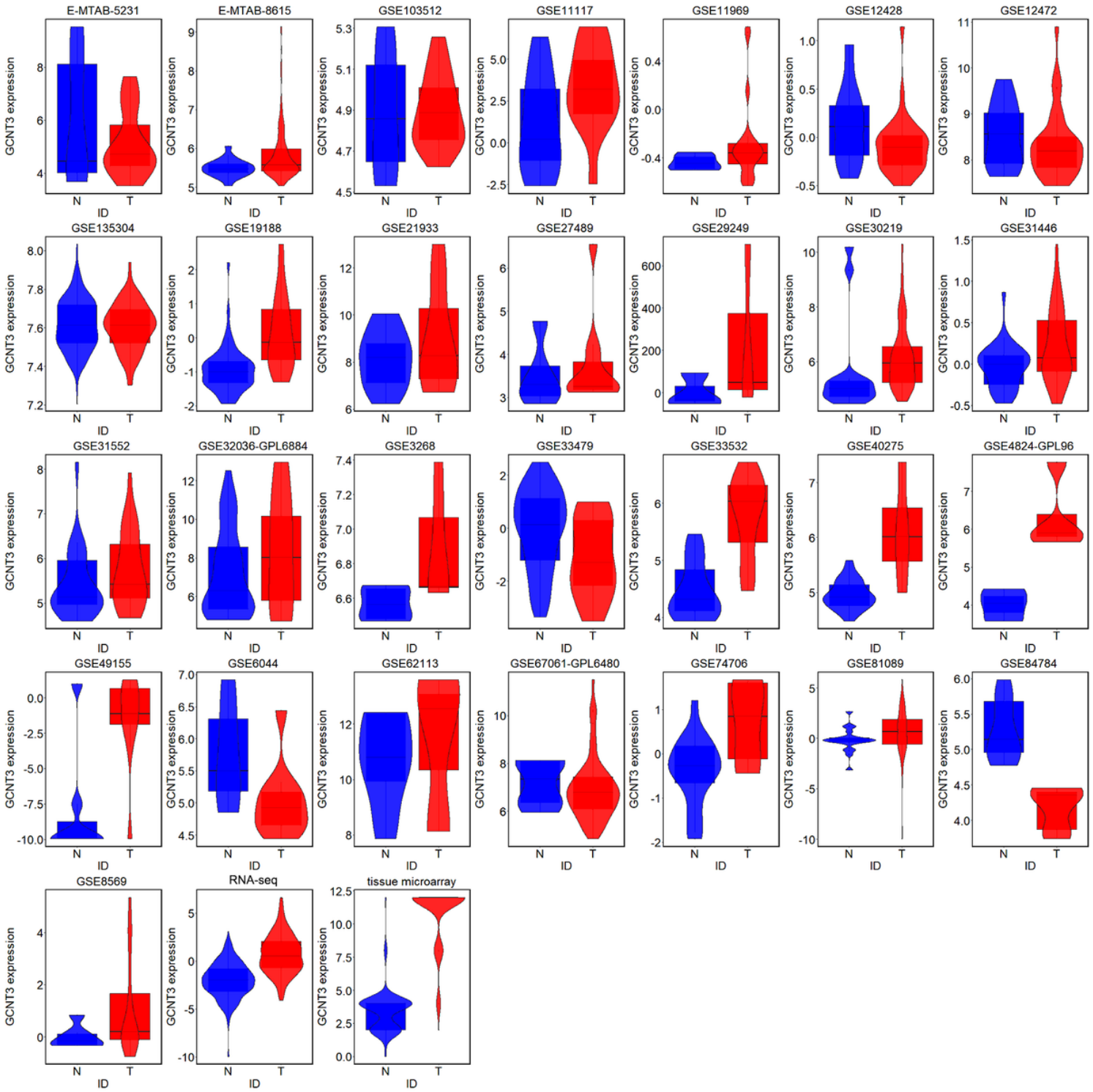

Figure 1

GCNT3 expression in lung squamous cell carcinoma and non-cancer samples from in-house tissue microarrays, external microarrays and RNA-seq dataset. N: non-cancer sample; T: lung squamous cell carcinoma sample.

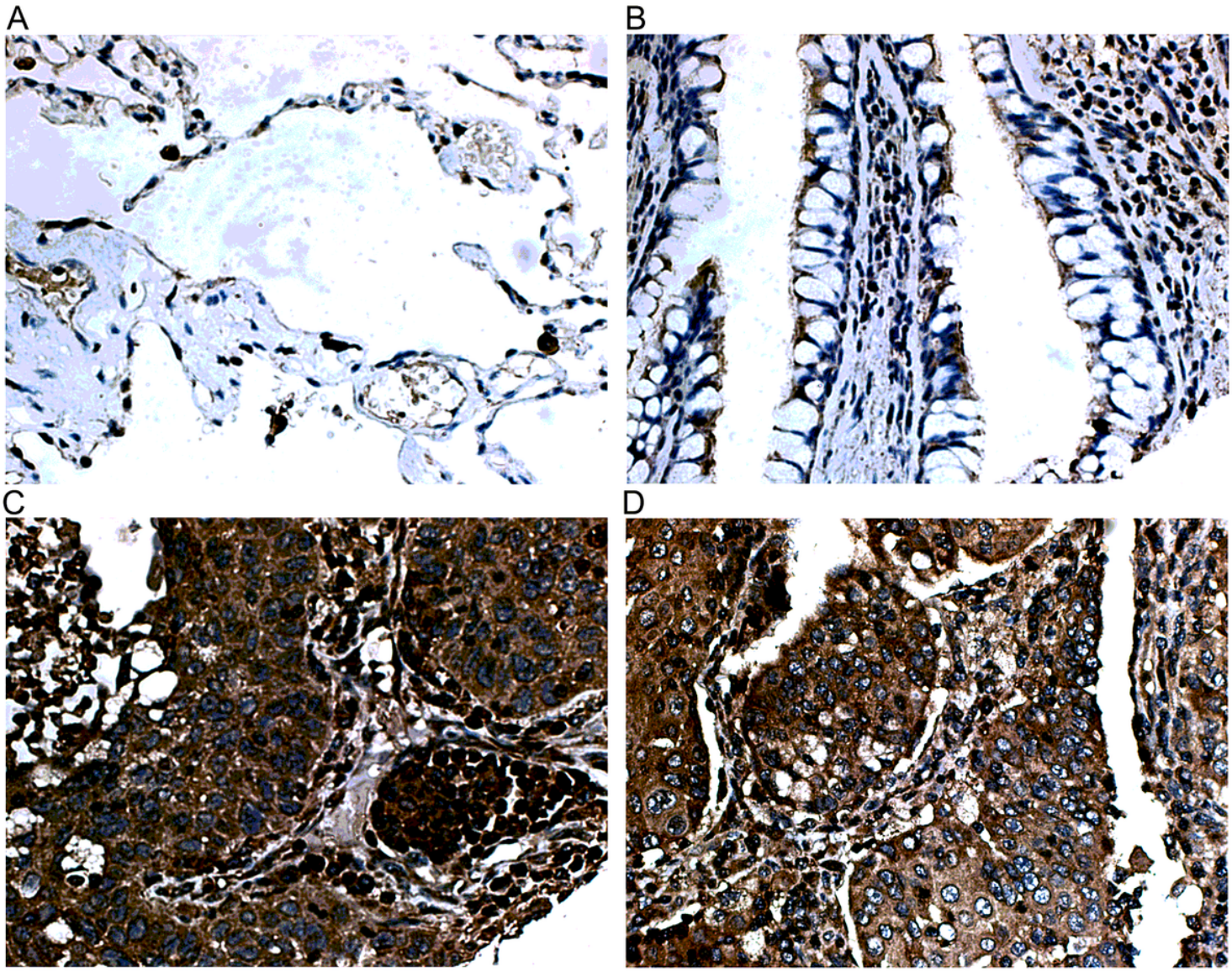

Figure 2

IHC staining of GCNT3 in lung squamous cell carcinoma and non-cancer tissues from tissue microarrays. A. Negative staining of GCNT3 in non-cancer pulmonary alveoli tissues (400x); B. Negative staining of GCNT3 in non-cancer bronchus tissues (400x); C. Strong staining of GCNT3 in lung squamous cell carcinoma tissues (400x); D. Strong staining of GCNT3 in lung squamous cell carcinoma tissues (400x).

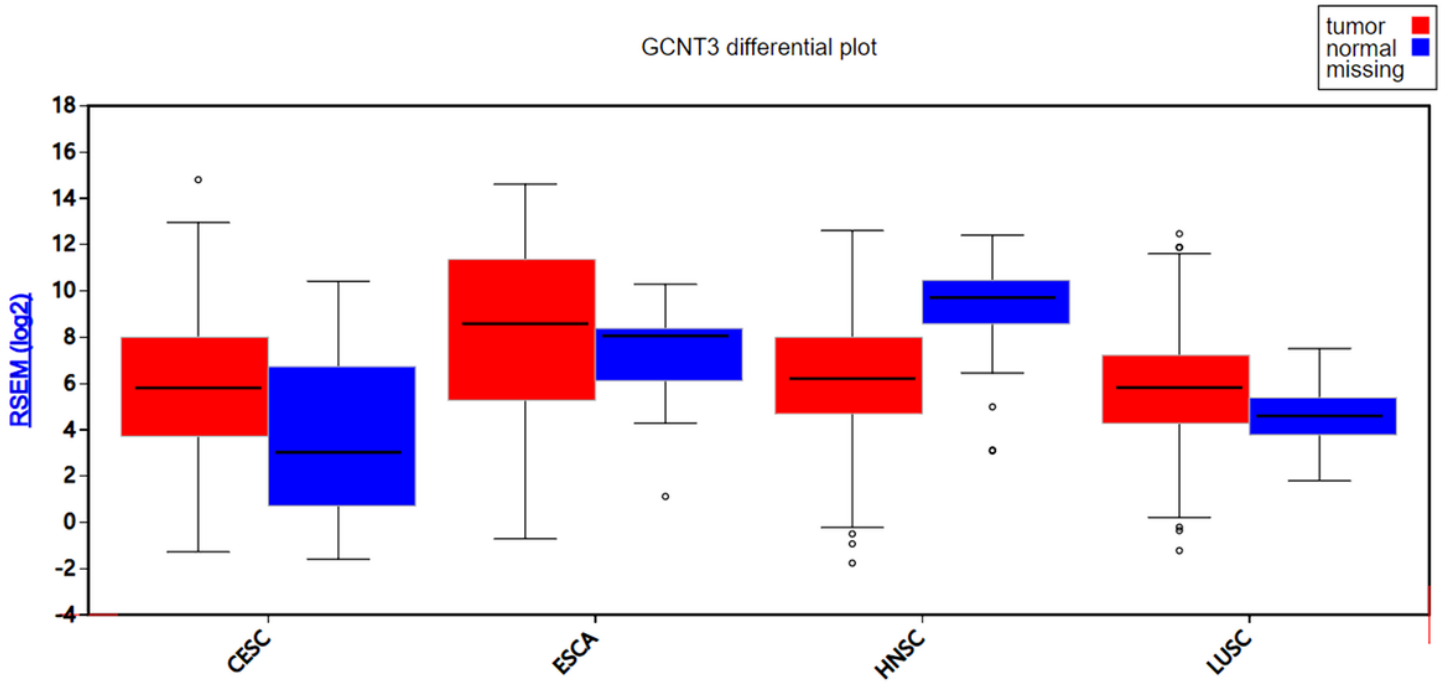

Figure 3

GCNT3 expression in pan-squamous cell carcinoma tissues. RSEM: RNA-Seq by expectation-maximization; CESC: cervical squamous cell carcinoma; ESCA: esophageal squamous cell carcinoma; HNSC: head and neck squamous cell carcinoma; LUSC: lung squamous cell carcinoma.

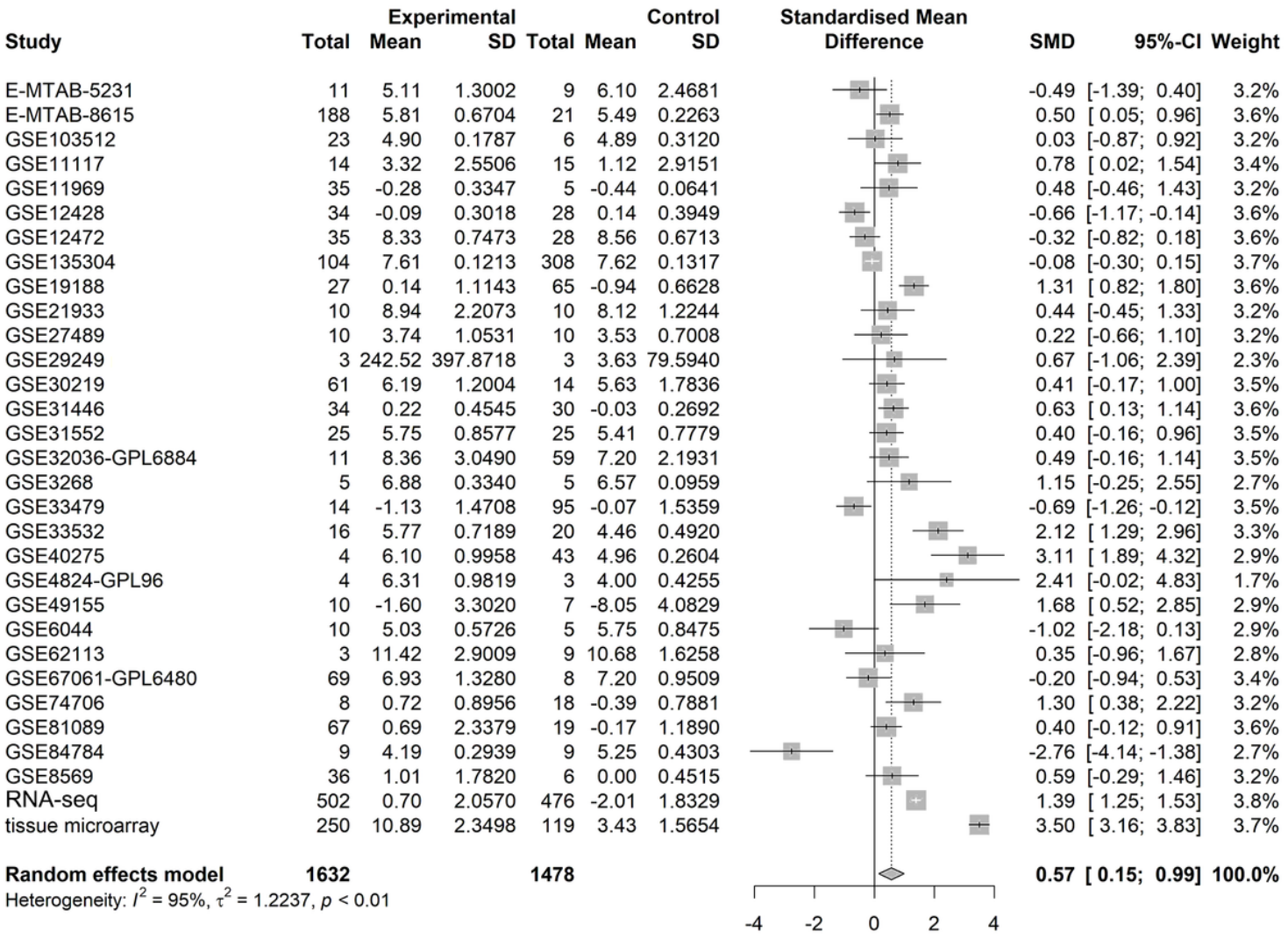

Figure 4

Pooled SMD forest plot of GCNT3 in lung squamous cell carcinoma for in-house tissue microarray, external microarrays and RNA-seq datasets. SMD: standard mean difference; SD: standard deviation.

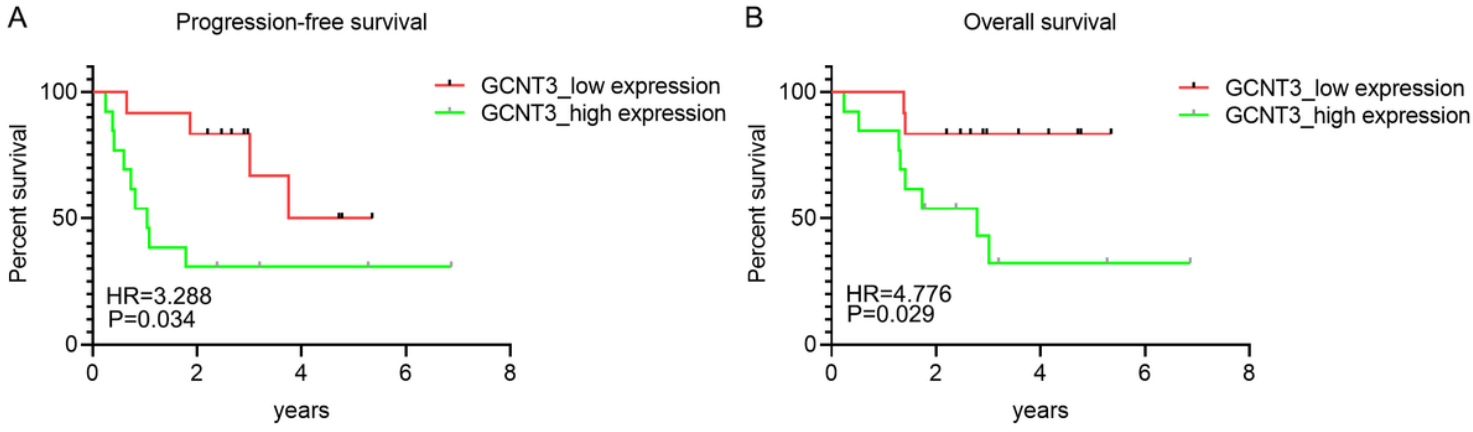

Figure 5

Survival analysis of GCNT3 expression in GSE29013 dataset. A. Kaplan-Meier survival curves for progression-free survival of lung squamous cell carcinoma patients from GSE29013; B. Kaplan-Meier survival curves for overall survival of lung squamous cell carcinoma patients from GSE29013. HR: hazard ratio.

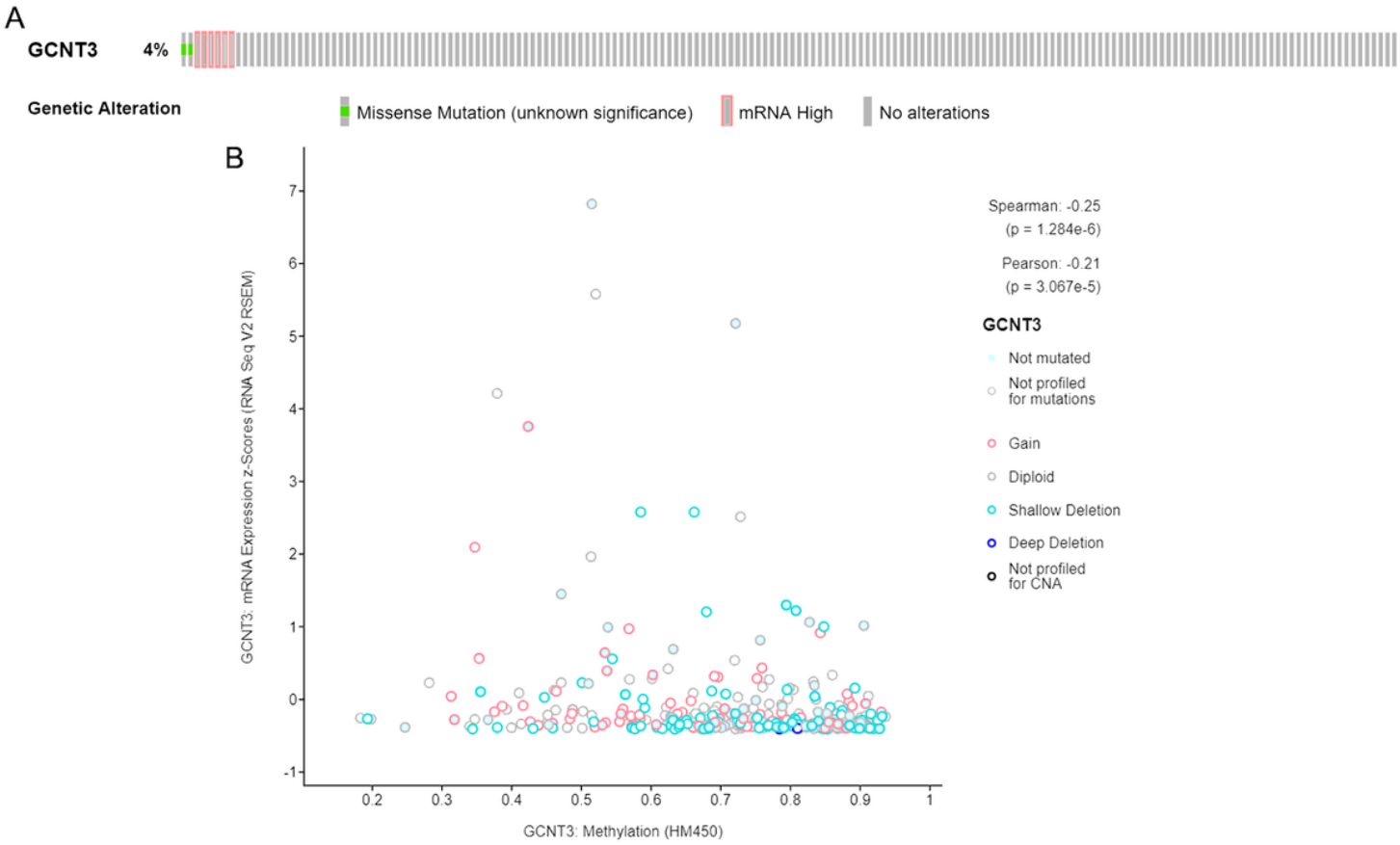

Figure 6

Genetic alteration and methylation level of GCNT3 in lung squamous cell carcinoma. A. Genetic alteration status of GCNT3 in 178 lung squamous cell carcinoma samples profiled in mRNA expression. B. Correlation daigram of methylation level and mRNA expression value of GCNT3 in lung squamous cell carcinoma.

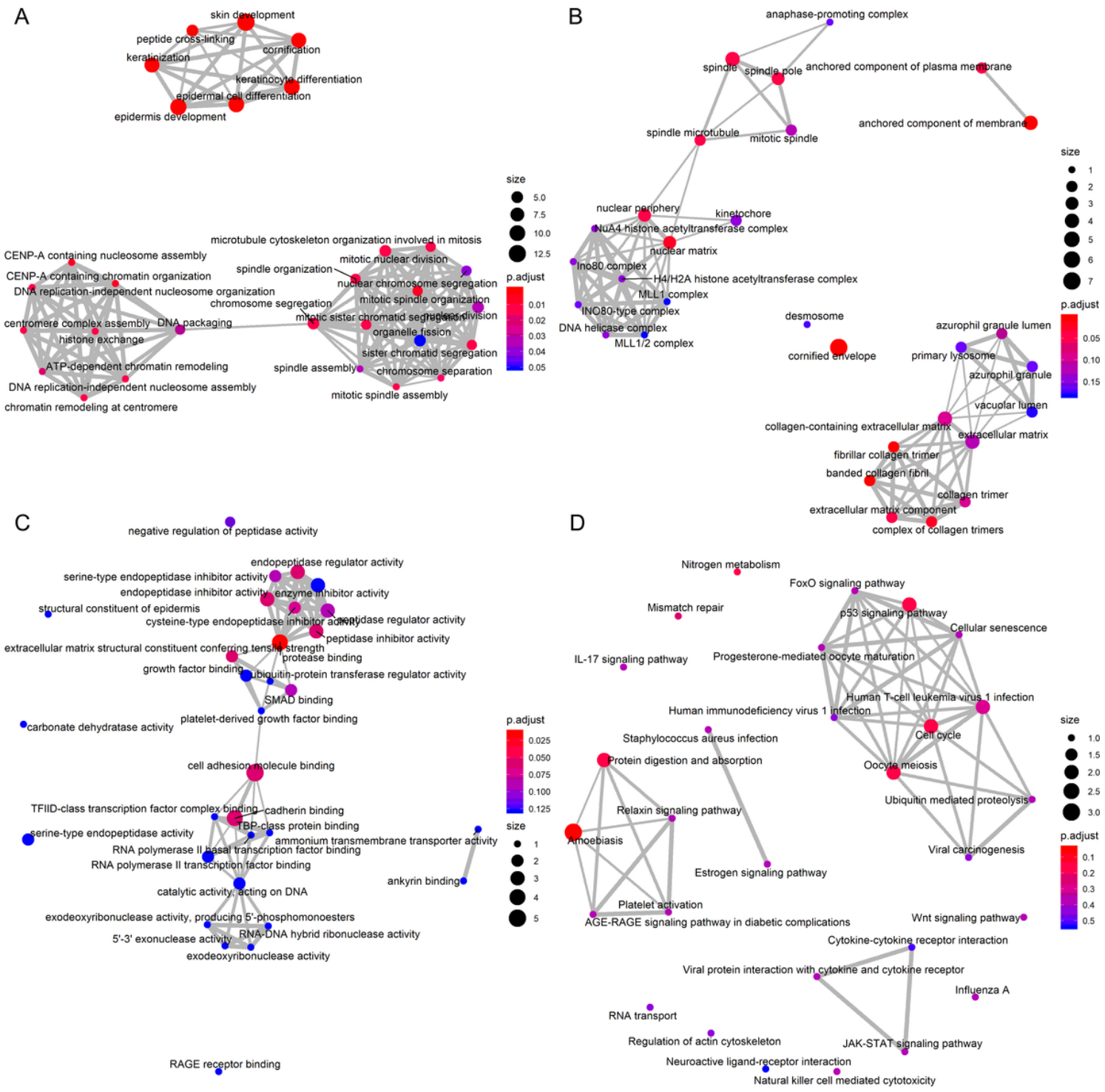

Figure 7

Functional enrichment analysis for genes positively correlated with GCNT3 in lung squamous cell carcinoma. A. Emapplot for biological process terms. B. Emapplot for cellular component terms. C. Emapplot for molecular function terms. D. Emapplot for pathway terms.

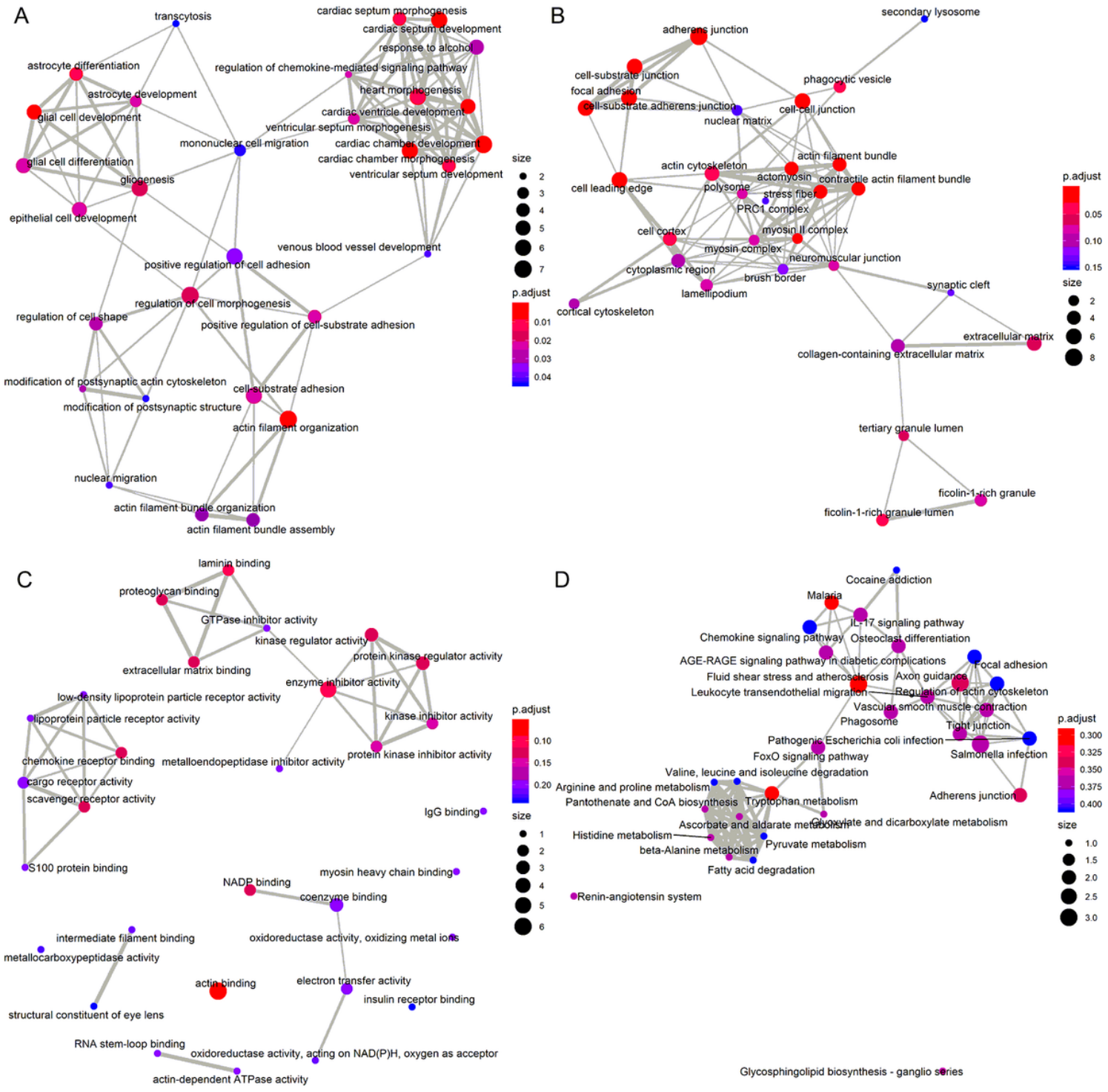

Figure 8

Functional enrichment analysis for genes negatively correlated with GCNT3 in lung squamous cell carcinoma. A. Emapplot for biological process terms. B. Emapplot for cellular component terms. C. Emapplot for molecular function terms. D. Emapplot for pathway terms.

Supplementary Files

This is a list of supplementary files associated with this preprint. Click to download.

- SupplementaryFigure1.tif
- SupplementaryFigure2.tif
- SupplementaryFigure3.tif
- SupplementaryFigure4.tif
- SupplementaryFigure5.tif
- SupplementaryTable1.docx